Virology 446 (2013) 303–313

Contents lists available at ScienceDirect

Virology

journal homepage: www.elsevier.com/locate/yviro

The interaction between claudin-1 and dengue viral prM/M protein for its entry

Pulin Che [a,b], Hengli Tang [c], Qianjun Li [a,b,*]

[a] Department of Microbiology, University of Alabama at Birmingham, Birmingham, AL 35294, United States
[b] University of Alabama at Birmingham, Department of Medicine, Division of Infectious Diseases, BBRB 562, 845 19th Street South, Birmingham, AL 35294, United States
[c] Department of Biological Science, Florida State University, 3063 King Life Sciences, Stadium Drive, Tallahassee, FL 32306, United States

ARTICLE INFO

Article history:
Received 28 June 2013
Returned to author for revisions
18 July 2013
Accepted 9 August 2013
Available online 7 September 2013

Keywords:
Dengue virus
Claudin-1
prM
Virus entry
Extracellular loops
Tight junction

ABSTRACT

Dengue disease is becoming a huge public health concern around the world as more than one-third of the world's population living in areas at risk of infection. In an effort to assess host factors interacting with dengue virus, we identified claudin-1, a major tight junction component, as an essential cell surface protein for dengue virus entry. When claudin-1 was knocked down in Huh 7.5 cells *via* shRNA, the amount of dengue virus entering host cells was reduced. Consequently, the progeny virus productions were decreased and dengue virus-induced CPE was prevented. Furthermore, restoring the expression of claudin-1 in the knockdown cells facilitated dengue virus entry. The interaction between claudin-1 and dengue viral prM protein was further demonstrated using the pull-down assay. Deletion of the extracellular loop 1 (ECL1) of claudin-1 abolished such interaction, so did point mutations C54A, C64A and I32M on ECL1. These results suggest that the interaction between viral protein prM and host protein claudin-1 was essential for dengue entry. Since host and viral factors involved in virus entry are promising therapeutic targets, determining the essential role of claudin-1 could lead to the discovery of entry inhibitors with attractive therapeutic potential against dengue disease.

© 2013 Elsevier Inc. All rights reserved.

Introduction

Dengue virus (DENV), a mosquito-transmitted single strand RNA virus including four serotypes (DENV-1,-2, -3 and -4), belongs to the genus *Flavivirus* in the family *Flaviviridae*. DENV causes a broad spectrum of clinical manifestations, ranging from mild febrile illness to life threatening dengue hemorrhagic fever (DHF) and dengue shock syndrome (DSS) (WHO, 2012). Each year, 2.5 billion people are under risk of DENV infection, with 50 million infections and 500,000 cases of severe dengue with over 5% case fatality rate (WHO, 2012). In the past two decades, all four serotypes DENV extended their distribution geographically and circulated around tropical and sub-tropical countries, including those in Southeast Asia, the Pacific, Africa, Eastern Mediterranean and the Americas (Guzman et al., 2010). Unfortunately, there are no effective antiviral drugs or licensed vaccine currently available against DENV, and dengue diseases become a huge public concern (Halstead and Deen, 2002).

The DENV ssRNA genome is approximately 11 kb in length (Kinney et al., 1997), embedded in a DENV particle which contains three structural proteins, the capsid (C), envelope (E) and membrane (M) proteins. M is derived from the precursor M protein (prM) via cleavage (Perera and Kuhn, 2008). An internal host derived lipid bilayer encloses an RNA–protein core consisting of genome RNA and C proteins (Kuhn et al., 2002; Perera and Kuhn, 2008). DENV virions attach to the host cell surface receptors/co-receptors and enter the cell via receptor-mediated endocytosis (Lindenbach and Rice, 2003; Mercado-Curiel et al., 2008; Stiasny et al., 2009; van der Schaar et al., 2008). Fusion between the viral and cellular membranes requires reassociation of the E protein on the viral surface to form a number of fusogenic trimers via an intermediate structure that consists of E dimers surrounding patches of exposed membrane (Yu et al., 2009; Zhang et al., 2004). Subsequently, the acidic environment of the endosomal vesicles triggers conformational changes in E protein, resulting in fusion of the viral and cellular membranes (Heinz and Allison, 2003). The nucleocapsid is then released into the cytoplasm, and the genomic RNA is translated into a single polyprotein precursor in the order of C-prM-E-NS1-NS2A-NS2B-NS3-NS4A-NS4B-NS5, which is processed to three structural and seven non-structural (NS) proteins. Virus assembly is initiated by forming immature particles in endoplasmic reticulum (Mackenzie and Westaway, 2001; Yu et al., 2008). The formation of intracellular prM/E heterodimers occurs rapidly after translation and is important for the assembly and secretion of immature virus particles. The 'pr' retention prevents

* Corresponding author at: University of Alabama at Birmingham, Department of Medicine, Division of Infectious Diseases, BBRB 562, 845 19th Street South, Birmingham, AL 35294, United States. Fax: +205 934 5600.
E-mail address: liq@uab.edu (Q. Li).

0042-6822/$ - see front matter © 2013 Elsevier Inc. All rights reserved.
http://dx.doi.org/10.1016/j.virol.2013.08.009

membrane insertion, suggesting that 'pr' is present on the virion in the trans-Golgi network to protect the progeny virus from fusion within the host cell (Yu et al., 2009). During maturation, 'pr' peptide is cleaved from prM, and resulting M protein remains in the mature particle as a transmembrane protein beneath the E protein shell (Yu et al., 2009, 2008; Zhang et al., 2003).

DENV entry is a complicated process requiring specific interactions between multiple cell surface proteins and viral proteins (prM/M and E). Cell surface proteins serving as receptors/co-receptors are crucial determinants of tissue tropism during DENV infection. Several cell surface proteins have been identified as receptors/co-receptors in different target cells, however, DENV receptors still remains largely undefined, mainly due to the complexity of different target cells and different virus serotypes (Bielefeldt-Ohmann et al., 2001; Diamond et al., 2000). Macrophages, monocytes, and dendritic cells have been proposed as primary target cells during DENV infection. The binding of E protein to dendritic cell specific ICAM-3 grabbing non-integrin (DC-SIGN) triggers the internalization of DENV into the cells (Lozach et al., 2005; Navarro-Sanchez et al., 2003; Tassaneetrithep et al., 2003). Meanwhile, the mannose receptor (MR) expressed on macrophages has been shown to mediate entry by all four DENV serotypes via binding to the E protein (Miller et al., 2008). Other cell surface proteins involved in DENV entry include APO B100 (Guevara et al., 2010), the chemokine receptors CXCR3 and CXCL10 (Ip and Liao, 2010), and stress proteins related to the heat shock family such as GRP78/Bip (Jindadamrongwech and Smith, 2004) and heat-shock protein 70 and 90 (HSP70/90) (Reyes-Del Valle et al., 2005; Reyes-del Valle and del Angel, 2004). In insect C6/36 cells, prohibitin (Kuadkitkan et al., 2010) and the 45-kD heat-shock related glycoprotein (Salas-Benito et al., 2007) have been shown involved in DENV entry. Nevertheless, the exact cell surface proteins serving as receptors/co-receptors for DENV entry is still not well defined. In the present study, we examined and characterized the essential role of claudin-1 during DENV entry.

Results

Identification of claudin-1 involvement during DENV viral lifecycle:

Virus entry requires the involvement of many host cell surface factors, including tetraspanin CD 81 (Bartosch et al., 2003; McKeating et al., 2004; Pileri et al., 1998), tight junction protein claudin-1 (Evans et al., 2007; Liu et al., 2009) and occludin (Liu et al., 2009; Ploss et al., 2009), and human scavenger receptor class B type 1 (SR-BI) (Bartosch et al., 2003; Scarselli et al., 2002). To examine the role of claudin-1 during dengue viral lifecycle, we first established a stable cell lines with the knockdown of claudin-1 using shRNA technique. Stable Huh 7.5 cell lines transfected with non-targeting shRNA (NT-shRNA) served as a control cell line, designated as RK1 cells. Cell line with knockdown of claudin-1 was designated as RK4 cells, and further verified by western blot (Fig. 1A) and immunofluorescent staining (Fig. 1B). The immunofluorescent staining of RK1 cells showed clearly observable claudin-1 expression along the cell surface (Fig. 1B, arrow pointed). Claudin-1 expression was significantly reduced in claudin-1 knockdown cells (designated as RK4 cells), as claudin-1 expression in most RK4 cells was hardly observed on the cell surface, or only faint and broken line of claudin-1 expression observed on the surface of a few cells (Fig. 1B). There were some background staining in the cytoplasm in RK4 cells, which were also observed in the RK1 cells, but was not significantly different. This was further confirmed in our western blot analysis showing that there was strong claudin-1 expression in the RK1 control cells, and with less than 10% claudin-1 expression in the RK4 cells (Fig. 1A).

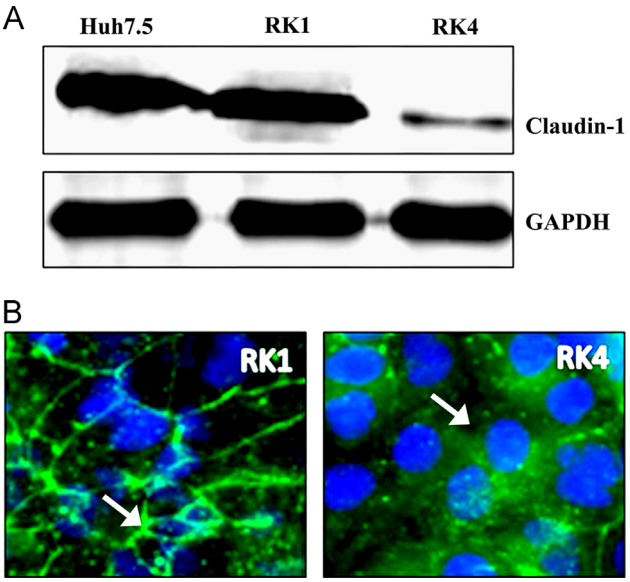

Fig. 1. The knockdown of claudin-1 expression in RK4 stable cell lines. Knockdown of claudin-1 in Huh 7.5 cells was carried out using claudin-1 specific shRNA, designated as RK4 cells. Cells tranfected with non-targeting shRNA (NT-shRNA) served as the control, designated as RK1 cells. (A) Western blot showing the reduction of claudin-1 expression in RK4 cells in comparison with that in the RK1 control cells and the original Huh 7.5 cells. GAPDH expression was also examined serving as loading control. (B) The expression of claudin-1 was disrupted in claudin-1 knockdown RK4 cells in comparison with that in the RK1 cells. Arrow in RK1 cells pointed to the claudin-1 expression around cells, whereas arrow in the claudin-1 knockdown RK4 cells showed that caludin-1 was depleted and there were only very little claudin-1 expression around the cell surface.

Knockdown of claudin-1 prevent DENV induced CPE

To investigate whether claudin-1 knockdown could affect DENV-induced CPE post infection, the dynamics of cell viability in claudin-1 knockdown RK4 cells was examined in comparison with that in the RK1 control cells after inoculated with DENV-2 at MOI of 1 using the previously established cell viability assay (Fig. 2A) (Che et al., 2009). Knockdown of claudin-1 strongly prevented DENV-2 induced CPE as we observed considerable increase of cell viability in claudin-1 knockdown RK4 cells comparing with that in Rk1 control cells. For instance, at 96 h.p.i., cell viability in control cells, including both Huh 7.5 and RK1 cells, were decreased to 18% and 15%, respectively. In claudin-1 knockdown Rk4 cells, cell viabilities were kept at high level, with about 66% cells viability at 96 h.p.i. (Fig. 2A). DENV-induced CPE was further examined under the phase contrast microscopic. In control RK1 cells, CPE was observed as early as 96 h.p.i., and became more pronounced at 120 h.p.i., respectively (Fig. 2D-b and -c). In claudin-1 knockdown RK4 cells, CPE was delayed and not observable at 96 h.p.i., (Fig. 2D-e) and only moderate CPE was observed at 120 h.p.i. (Fig. 2D-f). This observation further confirmed that DENV-2 induced CPE was prevented or delayed in claudin-1 knockdown RK4 cells. Furthermore, cell growth in RK4 cells was not affected due to the knockdown of claudin-1, since the cell growth rate in RK4 cells and the RK1 cells were identical (data not shown). The above results indicated that claudin-1 might play an essential role during DENV infection.

Furthermore, we also examined whether knockdown of claudin-1 could also protect CPEs induced by other DENV serotypes, including DENV-1, −3 and −4. Claudin-1 knockdown RK4 cells were infected with different DENV serotypes (DENV-1, DENV-3, DENV-4), and DENV induced CPE was evaluated at different h.p.i.. Interestingly, DENV-1 infection could not induce observable CPE in both RK1 and claudin-1 knockdown RK4 cells (results not shown). Both DENV-3 and DENV-4 induced CPE was inhibited in claudin-1 knockdown RK4

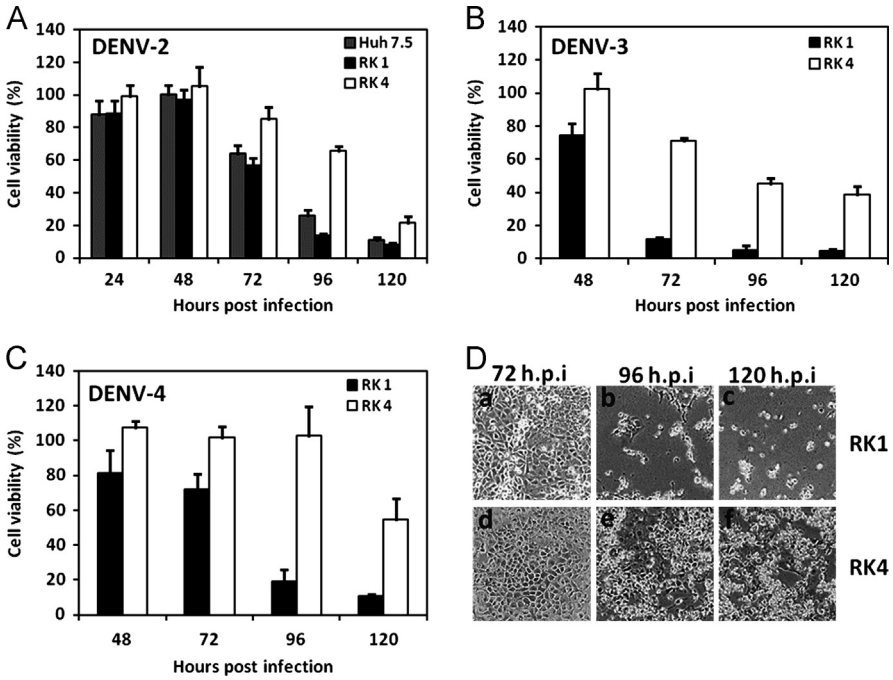

Fig. 2. DENV induced CPE and cell viability in different cell lines infected with different serotype of DENV. (A) Cell viability in claudin-1 knockdown RK4 cells, RK1 cells and Huh 7.5 cells at different h.p.i., after inoculated with DENV-2 at MOI of 1. (B) Cell viability post DENV-3 infection at MOI of 1 in claudin-1 knockdown RK4 cells and RK1 cells. (C) Cell viability post DENV-4 infection at MOI of 1 in claudin-1 knockdown RK4 cells and RK1 cells. Cell viability was assessed by the cell viability assay as described in the Methods and Materials. Data in each plot are representative of 3 separate experiments performed in triplicate. (D). Phase contrast images of a time-course of morphological changes observed in claudin-1 knockdown RK4 cells and RK1 control cells at different hours post DENV-2 infection at MOI of 1. All images were acquired at 100× magnification.

cells with up to 60% and 90% cell viabilities at 96 h.p.i., respectively (Fig. 2B and C). This was in agreement with the result when claudin-1 knockdown RK4 cells were infected by DENV-2, suggesting a potential of claudin-1 to serve as a common factor for different DENV serotypes. Collectively, these results demonstrated that loss of claudin-1 suppressed and delayed the development of DENV-induced CPE.

The possible role of claudin-1during DENV replication

Since knockdown of claudin-1 prevent DENV-2 induced CPE, we examined the dynamics of virus replication in claudin-1 knockdown RK4 cells in comparison with that in the RK1 control cells. Total RNAs were extracted from infected cells and culture medium at indicated h.p.i., respectively, followed by analyses of viral genomic RNA using qRT-PCR. Progeny virus production, expressing as PFU-equivalent RNA copies, in both cell and supernatant samples were examined in both RK1 and RK4 cells at 24 h intervals. Interestingly, we observed a log reduction of progeny virus production (RNA copies) in both cells and supernatant samples of the claudin-1 knockdown RK4 cells starting as early as 24 h.p.i., and remained at one log lower up till 96 h.p.i. (Fig. 3A and B). Although the progeny virus titer was lower in the RK4 knockdown cells, the replication dynamics was similar between the RK1 control and RK4 cells at different h.p.i.. This result was also confirmed when we determined the production of infectious progeny viral particles in claudin-1 knockdown RK4 cells using plaque assays. Similarly, we observed a consistent one to two logs reduction of virus titer in both cells and culture medium samples from the RK4 cells, respectively, in comparsion with that in the RK1 control cells (Fig. 3C and D). Similarly, the one-log difference in virus titer was observed as early as 24 h.p.i., and the virus replication dynamics kept in the similar fashion in both RK1 and RK4 cells. Collectively, the above results suggested that the effect of claudin-1 knockdown on DENV lifecycle might occurred before 24 h.p.i.. Similar phenomena were observed in the DENV-3 and -4 replication dynamics in RK4 knockdown cells (results not shown).

The effect of knockdown of claudin-1 using siRNA depletion

Due to the possible side effects associated with stable selection of cells expressing shRNA, we further analyzed the effect on DENV viral lifecycle in claudin-1 depleted cells using transient siRNA-mediated knockdown method. To deplete claudin-1 transiently, Huh 7.5 cells were transfected with 100nM human claudin-1 specific siRNA, and NT-siRNA transfection was utilized as control. The inhibition of claudin-1 expression was confirmed using western blot analysis (Fig. 4A). At 48 h post transfection, transfected cells were infected with DENV-2 at MOI of 1, and viral genomic RNA was determined using qRT-PCR at 24 h interval post infection. Consistent with the result in the shRNA knockdown stable cell lines, claudin-1 depleted cells showed an overall one-log reduction in viral RNA copies, but with similar virus replication dynamics when compared to that in the control cells (Fig. 4B). Collectively, both shRNA and siRNA mediated depletion of claudin-1 had showed similar effect on DENV replication dynamics as early as 24 h.p.i., further indicating that claudin-1 might be required for DENV early viral lifecycle.

Claudin-1 was involved in DENV entry

Our results showed that knockdown of claudin-1, using both shRNA or siRNA techniques, could prevent DENV-2 induced CPE and reduce DENV-2 progeny virus production. We next sought to investigate in which viral lifecycle stage claudin-1 was involved. During HCV infection, claudin-1 was utilized as a co-receptor for virus internalization (Evans et al., 2007), and our investigation showed that DENV-2 viral genomic RNA or progeny virus production were one log lower as early as 24 h.p.i.. Thus, we first examined whether DENV entry was affected in claudin-1 depleted cells post DENV-2 infection. Viral genomic RNA (vRNA) from infected cells was evaluated at

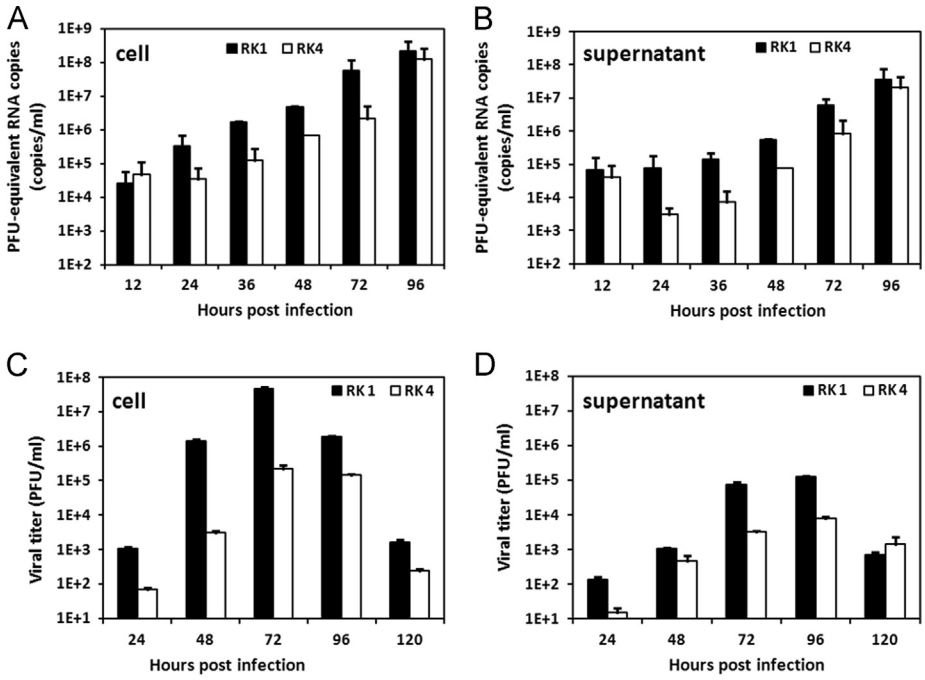

Fig. 3. Knockdown of claudin-1 expression affected DENV-2 viral life-cycle and reduced production of infectious progeny virus. Time course analysis of DENV genomic viral RNA, using qRT-PCR, in RK1 and RK4 cells (A) and supernatant (B) post DENV-2 infection at MOI of 1. Time-course analysis of progeny virus production in RK1 and RK4 cells (C) and supernatant (D) at different hours post DENV-2 infection as titrated by plaque assays. Results are expressed as mean ± S.D. of three separate experiments performed in duplicate.

different time post infection by focusing on the initial 12 h.p.i. (Fig. 4C). In comparison to control NT-siRNA cells, depletion of claudin-1 resulted in a significant decrease of DENV virus entry into the cells in the early stage of infection. At 2 h.p.i., there were only 50% virus entered into the knockdown cells when comparing with that in the control cells, and was consistent at 50% lower up to 8 h.p.i. The difference was even more pronounced at 10 h.p.i. and 12 h.p.i., as we observed over 60 and 80% reduction of viral genomic RNA in the knockdown cells, respectively. These results suggested that virus entry was hampered in claudin-1-depleted cells, suggesting that claudin-1 is required for efficient DENV entry.

To further confirm the involvement of claudin-1 during virus entry, we examined whether the entry of DENV-2 into the claudin-1 knockdown RK4 cells could be rescued by restoring claudin-1 expression in the cells. Claudin-1 knockdown RK4 cells were transiently transfected with plasmid DNA encoding wild-type human claudin-1. An empty vector was also used as negative control. In addition, RK1 control cells were also pre-treated with 1 μM compound 6, a known DENV entry inhibitor (Wang et al., 2009), as a positive control in inhibiting DENV entry. We first confirmed that claudin-1 was expressed in the transfected cells using western blot (Fig. 5A). We then confirmed that DENV-2 genomic RNA and progeny virus production in claudin-1 knockdown cells were reduced in the initial 12 h.p.i., similar to pattern observed in the claudin-1 depleted cells using siRNA knockdown (Fig. 5B).

The claudin-1 knockdown RK4 cells, transfected with human claudin-1 plasmid DNA or empty vector, were inoculated with DENV-2 (MOI of 1) at 48 h post transfection. Viral genomic RNA was then quantified at indicated time points using qRT-PCR. Notably, RK4 cells with restored claudin-1 expression showed increased virus entry into the cells at a level comparable to that in the control RK1 cells (Fig. 5B). On the other hand, the reduction of DENV virus entry in claudin-1 knockdown RK4 cells was comparable to that in RK1 cells treated with entry inhibitor, indicating DENV entry was impaired in claudin-1 knockdown RK4 cells. Similar phenomena were observed in the DENV-3 and -4 replication dynamics in RK4 knockdown cells (results not shown). Taken together, these data strongly suggested that claudin-1 might be essential for efficient DENV entry.

Interaction of claudin-1 with DENV viral protein

It was proposed that via interacting with viral protein, claudin-1 serves as a receptor for recruiting virions to cell surface during HCV entry (Cukierman et al., 2009; Evans et al., 2007; Meertens et al., 2008; Zheng et al., 2007). Since we showed that claudin-1 was also required for efficient DENV entry, we further analyzed whether claudin-1 interacted with DENV viral protein. During DENV infected cells, a larger precursor, PrM of approximately 19 kDa, is synthesized. DENV prM is further processed and cleaved into 'pr' and M proteins. DENV M is a small, approximately 10 kDa protein found in the mature virus particle. To determine the possible interaction of claudin-1 with DENV viral protein, we examined the direct binding between claudin-1 and viral glycoproteins prM. We used purified recombinant HIS-tagged prM protein as the bait to fish the protein extracts prepared from whole cell lysate of Huh 7.5 cells. We identified claudin-1 as one of the host proteins that interacted with prM protein (Fig. 6A). This interaction was further verified when purified GST-tagged claudin-1 efficiently interacted with HIS-tagged prM protein in the pull-down assay (Fig. 6B). Strikingly, a robust binding of claudin-1to 'pr', M and prM were also observed on our pull-down assay, however, viral E protein does interact with claudin-1 (Fig. 6C). This result suggested a direct interaction between claudin-1and prM, including pr, M and prM proteins.

ECL1 is essential for the interaction between claudin-1 and prM

Previous studies in HCV entry showed that either ECL1 or ECL2 is essential for the interaction of claudin-1 with viral protein. To further verify the interaction between prM and claudin-1 and to determine the essential domains in claudin-1 for the interaction, we constructed deletion mutants with either ECL1 or ECL2 deleted (Fig. 7A). These mutant proteins were expressed, purified and protein-protein interaction was analyzed using pull-down assays (Fig. 7B). When ECL1 was

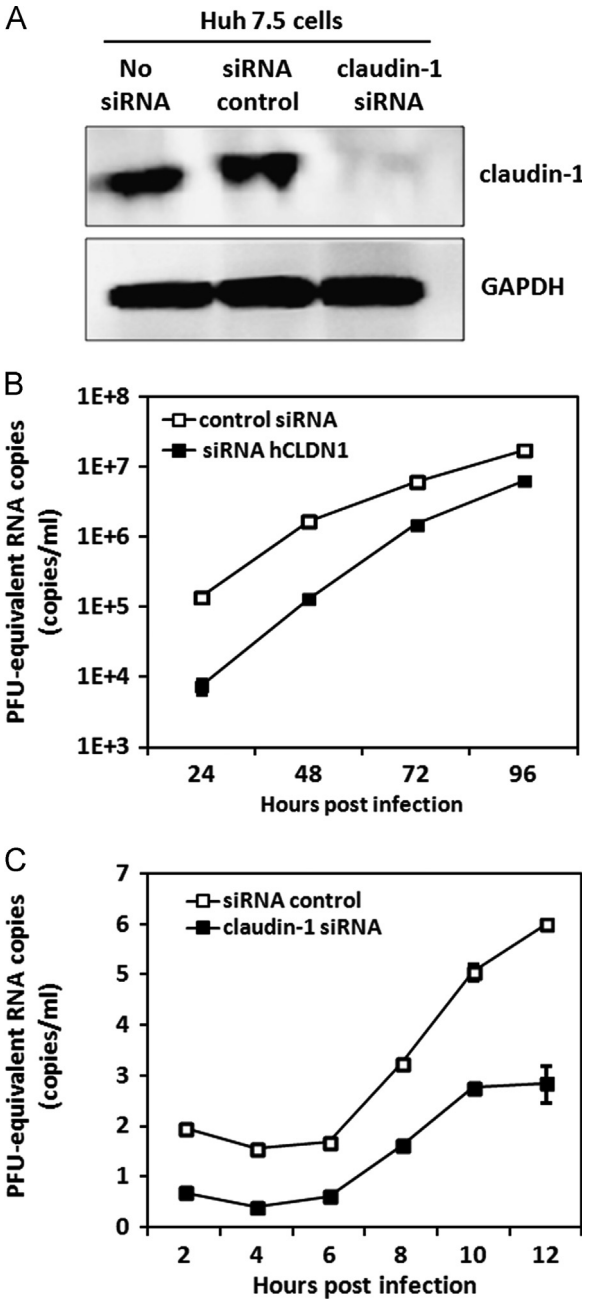

Fig. 4. The effect of claudin-1 depletion using claudin-1 specific siRNA. (A). Claudin-1 was depleted in Huh 7.5 cells using claudin-1 specific siRNA. Western blot analysis confirmed that claudin-1 expression was knockdown at the protein levels in comparison to scrambled siRNA control. (B) Time-course of DENV progeny virus production in claudin-1 depleted cells at 24 h interval at different h.p.i. PFU-equivalent viral RNA copies was determined by qRT-PCR. (C) DENV genomic RNAs in cell lysate were analyzed using qRT-PCR analysis. Samples were collected every 2 h in a time course manner for the initial 12 h.p.i.

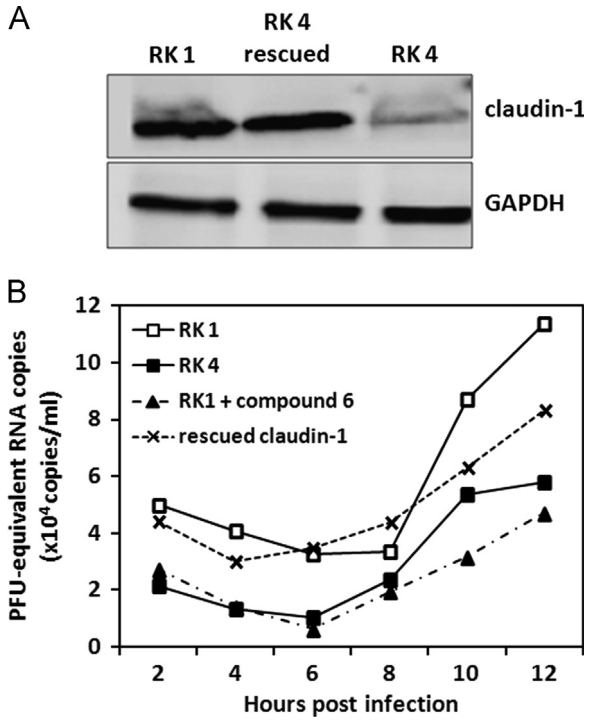

Fig. 5. Restoring claudin-1 expression in claudin-1 knockdown RK4 cells rescued DENV infection in the initial 12 h.p.i. Claudin-1 DNA was transfected into the claudin-1 knockdown RK4 cells. (A). The expression of claudin-1 was restored in RK4 cells transfected with plasmid DNA containing full length human claudin-1. (B). Time-course analysis of virus entering into the cells in the initial 12 h.p.i. in cells with or without human claudin-1transfection. Compound 6 at 1μM was used as a positive control.

deleted, the interaction between prM and claudin-1ΔECL1 was not observed as there was no detectable claudin-1ΔECL1 in the pull-down samples. The deletion of ECL2 did not affect the interaction as claudin-1ΔECL2 mutation could be pulled down by HIS-tagged prM protein, similar to that in the full length claudin-1. This result indicated that ECL1 was essential for the binding of claudin-1 with prM.

Determining the essential amino acids on the ECL1

Early studies showed that amino acids in highly conserved ECL1 motif, W_{30}-GLW_{51}-C_{54}-C_{64}, plays an important role in maintaining its 3D-structure and are important for HCV entry (Cukierman et al., 2009). Another amino acid, isoleucine at position 32 (I32), has been proposed to be involved in ion regulation, and early studies showed exchange of I32 to M (I32M) impaired HCV entry (Evans et al., 2007). Cysteine at position 54 and 64 are known to form disulfide bond in ECL1, which plays an important role in stabilizing ECL1 structure, suggesting the specific structure of ECL1 is required for robust binding. To determine the essential amino acids on the ECL1, a panel of seven point mutations on ECL1 was constructed by alanine substitution of the aforementioned 6 highly conserved amino acids on ECL1 motif, plus the exchange of isoleucine with methionine at position 32. Although ECL2 was not required for prM binding and not engaged in tight junction barrier regulation, we still selected 8 polar amino acids on ECL2 for alanine substitution, including T137, Y140, Q146, Y149, T153, N156, Y159, and Q163. Each point mutation was constructed by site-directed mutagenesis, and the respective recombinant proteins were expressed and purified as described in method section. The interaction of these claudin-1 mutants with prM protein was examined using the pull-down assay. Our results showed that only C54A, C64A and I32M mutations on ECL1 impaired the claudin-1-prM interaction (Fig. 8A), whereas none of the other mutations on ECL1 and ECL2 showed any effect on claudin-1-prM interaction (Fig. 8B). Altogether, above data revealed an essential interface on ECL1 of claudin-1, which might be required for efficient virus-host interaction.

Discussion

In this study, we showed that claudin-1, the major structural component of tight junction, was involved in DENV entry by directly interacting with viral prM protein. Tight junction is an intercellular junctional structure, which functions as a physical barrier with

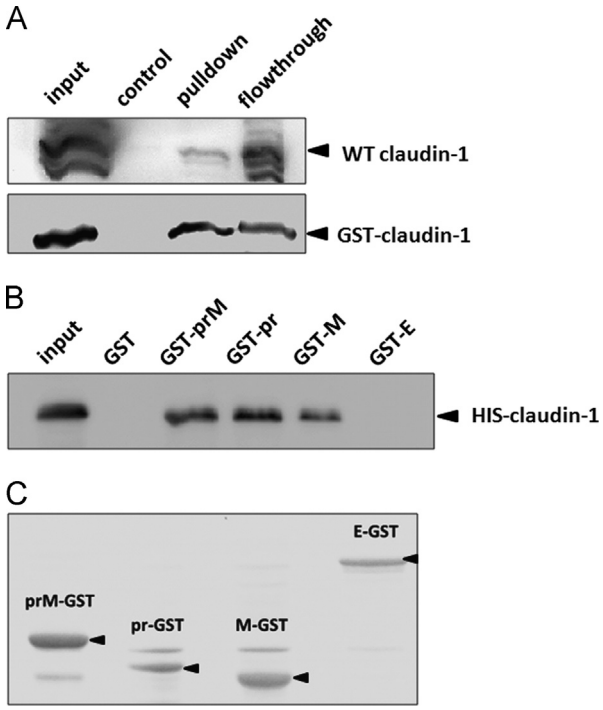

Fig. 6. The interaction between claudin-1 and DENV viral proteins. (A) Direct interaction between purified HIS-tagged prM and wild type claudin-1 from cell lysate or semi-purified GST-tagged claudin-1 via pull-down assay. Semi-purified HIS-tagged prM protein was used as the bait. The input lane indicates wt claudin-1 in the original cell lysate, and the control lane showed that no wt claudin-1 was pulled down using empty nickel chelate beads. (B). Direct interaction between purified HIS-tagged prM and purified GST-tagged claudin-1 via pull-down assay. Purified HIS-tagged prM protein was used as the bait. The input lane indicates purified GCT-tagged claudin-1 input, and the control lane showed that no purified claudin-1 was pulled down using empty nickel chelate beads. (C).The semi-purified HIS-tagged claudin-1 interacted with semi-purified GST-tagged prM, M and pr, but not the GST-tagged E protein. Input lane indicates the original semi-purified HIS-tagged claudin-1. GST protein was used as negative control. For the above experiment, claudin-1 was detected by western blot analysis using anti-claudin-1 antibody.

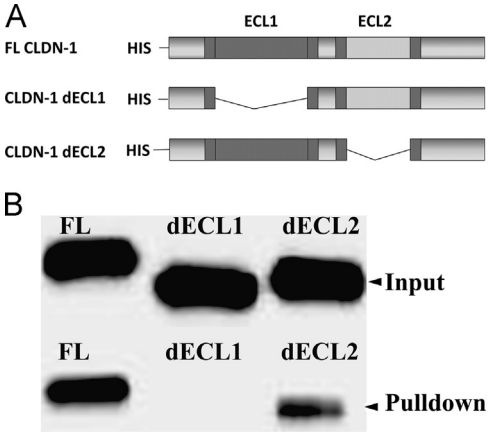

Fig. 7. Effect of ECL1 or ECL2 deletion on the interaction between Claudin-1 and prM (A) Illustration of the construction of claudin-1 ECL1 and/or ECL2 domain deletion mutants with HIS-tagged. (B) Protein–protein interaction between GST-tagged prM and HST-tagged claudin-1 ECL1 or ECL2 deletion mutations, analyzed using pull-down assay. The HIS-tagged claudin-1 ECL1 mutant cannot pull-down HIS-tagged prM protein, whereas there is no effect when ECL2 was deleted.

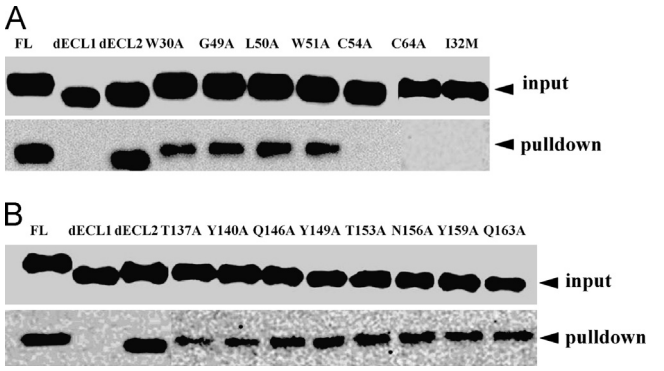

Fig. 8. The interaction between HIS-tagged prM and point mutations of claudin-1. Mutagenesis in both ECL1 and ECL2 were shown with critical residues in the ECL1 and ECL2 of claudin-1 being replaced by alanine. In both figures, the input lane indicates the initial full-length claudin-1 used for the assay. The input for other deletion and mutation proteins were the same as the full-length claudin-1, hence, were not shown here. (A). The interaction of point mutation in ECL1 domain with GST-tagged prM protein was analyzed. The HIS-claudin-1 ECL1 and ECL2 deletion mutation were included as positive and negative controls. Top panel showed the amount of input proteins for full-length protein, ΔECL1, ΔECL2 and each mutation, while the bottom panel showed the actually pull down. (B). The interaction of point mutation in ECL2 domain with GST-tagged prM protein was analyzed. The HIS-claudin-1 ECL1 and ECL2 deletion mutation were included as positive and negative controls. Top panel showed the amount of input proteins for full-length protein, ΔECL1, ΔECL2 and each mutation, while the bottom panel showed the actually pull down.

extremely small openings, allowing the passage of nano-sized or even smaller molecules and restricting the penetration of macro-materials and microbes (Lorenza González-Mariscal and Bautista). Disruption of tight junction contributes to pathogenesis. Extensive disruptions in tight junctions integrity and altered expression and distribution of claudins have been observed in infections of enteropathogenic *Escherichia Coli* (EPEC) (Guttman et al., 2006; Yuhan et al., 1997), *H. pylori* infection (Fedwick et al., 2005), *S. flexneri* (Sakaguchi et al., 2002), rotavirus (Dickman et al., 2000; Nava et al., 2004; Obert et al., 2000), influenza virus (Armstrong et al., 2012), and HIV-1 virus (Andras and Toborek, 2011). On the other hand, pathogens, especially viruses, have evolved strategies to utilize tight junction to gain access into cells. *Clostridium perfringens* enterotoxin binds directly to the second extralcellular loop on claudin-3, -4 to gain access into cells (Fujita et al., 2000; Sonoda et al., 1999; Takahashi et al., 2005; Van Itallie et al., 2008). claudin-1, -6, -9 and occludin (Benedicto et al., 2009; Liu et al., 2009; Ploss et al., 2009) have been reported as co-receptors for HCV entry (Evans et al., 2007; Meertens et al., 2008; Zheng et al., 2007). Our data showed that depletion of claudin-1 expression hampered DENV-2 entry, reduced progeny virus production and prevent DENV-2 induced CPE. These results strongly suggested that claudin-1 was utilized by DENV-2 to facilitate its entry, which is in agreement with the observation during the entry of other viruses, including HCV (Gao et al., 2010; Harris et al., 2010; Liu et al., 2009; Meertens et al., 2008).

Claudin-1 has been shown to serve as a co-receptor for HCV entry, and deletion of ECL1 or mutation of in highly conserved amino acid W_{30}-GLW$_{51}$-C$_{54}$-C$_{64}$ on ECL1 motif hampered the HCV entry (Cukierman et al., 2009). The present study also identified ECL1 as the essential domain for its interaction with DENV prM protein. However, we only identified C_{54} and C_{64} as the essential amino acids, but not W_{30}, G, L, and W_{51}. We also identified I32 as the essential amino acid for binding activity. Prior studies suggested that ECL1 regulates the paracellular permeability and ion selectivity, while ECL2 is required for interactions between different claudin isoforms which is the linkage between adjacent cells (Van Itallie and Anderson, 2006). The two cysteines may form an intracellular disulfide bond in ECL1 (Li et al., 2013), a proposed key determinant in pore formation. The disulfide bonds between the two cysteines are critical in maintaining proper folding and stability (Doig and Williams, 1991; Taniyama et al., 1991). Notably, these two cysteines are conserved among all claudin isoforms and are critical in regulating tightness function (Krause et al., 2008;

Wen et al., 2004). Studies using claudin-1_{53-80} peptide, which contains C54 and C64, showed disrupted barrier function both in vitro and in vivo (Mrsny et al., 2008). In addition, introduction of I32M into ECL1 also disrupted protein binding. This is in agreement with Evans et al., when introduction of M32I into claudin-7 could render T293 cells partially permissive to HCVpp (Evans et al., 2007), whereas the wt claudin-7 expression on T293 failed to render it permissive. It is known that residue I32 may be involved in regulating the cation passage in tight junction. Since ECl2 was not involved in the interaction between prM and claudin-1, and it was not surprised that deletion of ECL2 or point mutation on ECL2 has no effect on the claudin-1 binding activity.

It is interesting that up to 30% dengue virus secreted from mammalian or insect cells are immature virus particles, with intact prM protein on the virus particle surface (Murray et al., 1993; Rodenhuis-Zybert et al., 2010; Wang et al., 1999; Zybert et al., 2008). In the immature virus, prM and E form heterodimers, protruding from virus surface as 60 trimeric spikes. The pr peptide caps the fusion loop of E protein, prevent the low-pH driven conformational change and pre-membrane fusion before virus release (Heinz and Allison, 2003; Lindenbach and Rice, 2003). The 'pr' peptide caps the fusion loop of E protein and prevent conformational change of E protein which is required for subsequent membrane fusion (Yu et al., 2008; Zybert et al., 2008). This is evidenced by inefficient infectivity and high percentage of immature progeny virus in both mammalian and insect cells. Recently, it has been reported that during entry step, the pr-capped fusion loop of E protein could be cleaved by furin, allowing conformational change and fusion of E protein, which renders immature virus infectious (da Silva Voorham et al., 2012; Rodenhuis-Zybert et al., 2011). In the present study, our data provide supporting evidence that immature particles can also interact with claudin-1 protein on the cell surface, and might be capable to entry into the target cells via this interaction. This result is also in agreement with the conclusion of Gao et al. that prM is required for an efficient entry(Gao et al., 2010). Further investigations will be needed to explore how immature virus particles interact with cell surface proteins to entry the target cells, and to understand whether claudin-1 is able to trigger the endocytosis or only plays a role in mediating virus attachment.

Viral entry is initiated by virus attachment, followed by rolling over the cell surface until endocytosis occurs. Apically resided tight junctions provide an ideal "trap" for the viruses. It is possible that the interaction between cell surface protein claudin-1 and viral prM/M could help to concentrate viruses at tight junction. These locally concentrated viruses may promote contact with other cell surface proteins served as receptors/co-receptors, including direct binding between HCV and claudin-1 ECL1 (Cukierman et al., 2009; Evans et al., 2007), HCV and occludin (Benedicto et al., 2009; Liu et al., 2010; Liu et al., 2009; Ploss et al., 2009), and between *Clostridium perfringens* enterotoxin and ECL2 on claudin-3 and -4 (Fujita et al., 2000; Takahashi et al., 2005; Van Itallie et al., 2008). Nevertheless, our data present here provided new evidence on the interaction between claudin-1 and prM during DENV entry, expanding our knowledge to understand in the essential role of claudin-1 for DENV infection.

Material and method

Cells and viruses

Cells were maintained in Dulbecco's modified Eagle's medium (DMEM) (Gibco BRL, Grand Island, NY) supplemented with 100 U/ml penicillin-streptomycin (P/S) (Invitrogen, Carlsbad, CA), 5% or 10% fetal bovine serum (FBS) (Invitrogen, Carlsbad, CA) for BSR and Huh 7.5, respectively. Cells were incubated at 37 °C, with 5% CO_2 and 80–95% humidity. Dengue virus serotype-1 (DENV-1) strain Hawaii, serotype-2 (DENV-2) strain 16681, serotype-3 (DENV-3) strain H87, serotype-4 (DENV-4) strain H241 were used in the current study. Virus stocks were prepared by inoculating Huh 7.5 cell monolayers at a multiplicity of infection (MOI) of 0.4. At 96 h post infection (h.p.i.), supernatants were collected and saved. Infected cells were harvested by gentle scraping, followed by three rapid freeze-thaw cycles in a dry-ice/ethanol bath. Cell debris was removed by centrifugation at 2000*g* for 10 min. Viral supernatant was collected, combined, aliquoted and stored at -80 °C. Virus titer was determined using a plaque assay on BSR monolayers in 24-well plates.

Plasmids construct

Vector pGEX-4T3 (Amersham Pharmacia, Piscataway, NJ) and pTriEx-4 (Novagen, Madison, WI, USA) were used for expression of recombinant proteins with GST tag or HIS tag, respectively. To obtain HIS tagged recombinant proteins, full length prM, pr, and M genes were cloned into Bam HI and Eag I REN (restriction enzyme) sites. Claudin-1gene was cloned into the Bam HI and Xho I REN sites on pTriEx-4 vector. To obtain GST tagged recombinant proteins, full length prM, pr, and M genes were cloned into Bam HI and Eag I REN sites; and claudin-1 was introduced into BamH I and Xho I REN sites on pGEX-4T3 vector, respectively. Deletion mutations (dECL1, dECL2) and point mutations were constructed using PCR-mediated overlap extension method to delete or mutate respective genes with sets of primers for each deletion/point mutation described in the following (Table 1) (Heckman and Pease, 2007). The sequence of each construction was confirmed by sequencing analysis at Heflin sequencing center at University of Alabama at Birmingham.

siRNA transfection

The siRNA is targeting nucleotides 5'-AAGTGAAGAGTA-CATGGCTGC-3' of claudin-1. The control or scrambled siRNA has a target sequence of 5'-GCGCGCTTTGTAGGATTCG-3'. Double-stranded siRNAs were constructed by in vitro transcription with a Silencer siRNA construction kit (Ambion, Austin, Tex.). Transfection of siRNA was performed using Oligofectamine (Invitrogen, Carlsbad, Calif.). Two days after transfection of siRNA, the cells were infected with DENV with MOI of 1.0.

Stable expression of shRNA using a lentiviral vector

The stable cell lines expression of different shRNAs were established using a lentiviral as described previously (Waninger et al., 2004). Briefly, the target sequences for claudin-1 and the scrambled shRNA were introduced into the U6 promoter/hairpin shRNA expression cassettes using the U6 promoter in pSilencer (Ambion). The cassettes were inserted into the pHIV-7-Puro vector, respectively. VSV-G-pseudotyped lentivirus was packaged using the lentivirus support kit (Invitrogen). Huh 7.5 cells were transduced by standard methods and subjected to selection with puromycin (0.6 μg/ml) for 10 days.

Plaque assay

Virus titer was determined using a plaque assay as described previously(Che et al., 2009). Briefly, BSR cells were seeded in 24-well plate and were inoculated with 10-fold serially-diluted virus. After inoculation, cells were incubated in 37 °C for 4 h for adsorption. The inoculum was removed and cells were washed with PBS twice. An overlay of 1% low-melting-point agarose

Table 1
List of primers used for construction of claudin-1 deletion and point mutants.

Primer ID	Sequence	Vector
Forward primer for prM	CGCGGATCCGTTCCATTTAACCACACGCAAT	Vector pTriEx-4
Reverse primer for prM	TAACGGCCGTTATGTCATTGAAGGAGC	
Forward primer for pr	ATTCGGCCGCACAGCTGTATACACGTGCA	
Reverse primer for pr	TAACGGCCGTTATCTTTTTTCTCTTCTATGTTC	
Forward primer for M	CGCGGATCCGTCAGTGGCACTCGTTCCACA	
Reverse primer for M	GCGGGATCCACGAGCTCAGATATCGTTGAGGA	
Forward primer for prM	CGCGGATCCTTCCATTTAACCACACGTAA	pGEX-4T3
Reverse primer for prM	TAACGGCCGTTATGTCATTGAAGGAGTGACAG	
Forward primer for pr	CGCGGATCCTTCCATTTAACCACACGTAA	
Reverse primer for pr	TAACGGGCCGTTATCTTTTTTCTCTTCTATGTTC	
Forward primer for M	CGCGGATCCTCAGTGGCACTCGTTCCACAT	
Reverse primer for M	TAACGGCCGTTATGTCATTGAAGGAGTGACAGC	
Forward primer for CLDN1/dEL1/dEL2	CGCGGATCC ATGGCCAACGCGGGGCTGCA	
Reverse primer for CLDN1/dEL1/dEL2	CCGCTCGAG TCACACGTAGTCTTTCCCGCT	
Reverse primer for fragment dEL1	TCCGTGCCCACCACTGGGGCAGGGCAGTGC	
Forward primer for fragment dEL1	TGCCCCAGTGGACCCGTGCCTTGATGGTGGT	
Reverse primer for fragment dEL2	TCGGACTGGTGCTGTGGCAACTAAAATAG	
Forward primer for fragment dEL2	TGCCACAGCAGGTCAGGCTCTCTTCACTGG	
Forward primer for CLDN1/dEL1/dEL2/point mutations	CGCGGATCCAATGGCCAACGCGGGGCTGCA	pTriEx-4
Reverse primer for CLDN1/dEL1/dEL2/point mutations	CCGCTCGAGTCACACGTAGTCTTTCCCGCT	
Reverse primer for CLDN1-W30A	GGAGTAAATCCTAGCCTGGGGCAGGGCAGTGCTGACGATG	
Forward primer for CLDN1-W30A	CAGGCTAGGATTTACTCCTATGCCGGCGACAACATCGTGACC	
Reverse primer for CLDN1-G49A	CATCCACAGAGCCTCGTACATGGCCTGGGCGGTCACGATGTTGTC	
Forward primer for CLDN1-G49A	ATGTACGAGGCTCTGTGGATGTCCTGCGTGTCGCAGAGCAC	
Reverse primer for CLDN1-L50A	GGACATCCAAGCCCCCTCGTACATGGCCTGGGCGGTCACGATG	
Forward primer for CLDN1-L50A	TACGAGGGGGCTTGGATGTCCTGCGTGTCGCAGAGCACCGGGC	
Reverse primer for CLDN1-W51A	GCAGGACATAGCCAGCCCCTCGTACATGGCCTGGGCGGTCACGATG	
Forward primer for CLDN1-W51A	GAGGGGCTGGCTATGTCCTGCGTGTCGCAGAGCACCGGGCA	
Reverse primer for CLDN1-C54A	CTGCGACACAGCGGACATCCACAGCCCCTCGTACATGGCCT	
Forward primer for CLDN1-C54A	TGGATGTCCGCTGTGTCGCAGAGCACCGGGCAGATCCAGTG	
Reverse primer for CLDN1-C64A	AAAGACTTTAGCCTGGATCTGCCCGGTGCTCTGCGACACGC	
Forward primer for CLDN1-C64A	CAGATCCAGGCTAAAGTCTTTGACTCCTTGCTGAATCTGAG	
Reverse primer for CLDN1-I32M	ATAGGAGTAGATCCTCCACTGGGGCAGGGCAGTGCTGACGATGGC	
Forward primer for CLDN1-I32M	CAGTGGAGGATGTACTCCTATGCCGGCGACAACATCGTGAC	
Reverse primer for CLDN1-T137A	ATACCATGCAGCGGCAACTAAAATAGCCAGACCTGCAAGAA	
Forward primer for CLDN1-T137A	TTAGTTGCCGCTGCATGGTATGGCAATAGAATCGTTCAAGA	
Reverse primer for CLDN1-Y140A	TCTATTGCCAGCCCATGCTGTGGCAACTAAAATAGCCAGAC	
Forward primer for CLDN1-Y140A	ACAGCATGGGCTGGCAATAGAATCGTTCAAGAATTCTATGA	
Reverse primer for CLDN1-Q146A	ATAGAATTCAGCAACGATTCTATTGCCATACCATGCTGTGG	
Forward primer for CLDN1-Q146A	AGAATCGTTGCTGAATTCTATGACCCTATGACCCCAGTCAA	
Reverse primer for CLDN1-Y149A	CATAGGGTCAGCGAATTCTTGAACGATTCTATTGCCATACC	
Forward primer for CLDN1-Y149A	CAAGAATTCGCTGACCCTATGACCCCAGTCAATGCCAGGTA	
Reverse primer for CLDN1-T153A	ATTGACTGGAGCCATAGGGTCATAGAATTCTTGAACGATTC	
Forward primer for CLDN1-T153A	GACCCTATGGCTCCAGTCAATGCCAGGTACGAATTTGGTCAGGC	
Reverse primer for CLDN1-N156A	GTACCTGGCAGCGACTGGGGTCATAGGGTCATAGAATTCTT	
Forward primer for CLDN1-N156A	ACCCCAGTCGCTGCCAGGTACGAATTTGGTCAGGCTCTCTT	
Reverse primer for CLDN1-Y159A	ACCAAATTCAGCCCTGGCATTGACTGGGGTCATAGGGTCAT	
Forward primer for CLDN1-Y159A	AATGCCAGGGCTGAATTTGGTCAGGCTCTCTTCACTGGCTGG	
Reverse primer for CLDN1-Q163A	GAAGAGAGCAGCACCAAATTCGTACCTGGCATTGACTGGGG	
Forward primer for CLDN1-Q163A	GAATTTGGTGCTGCTCTCTTCACTGGCTGGGCTGCTGCTTC	

(Invitrogen, Carlsbad, CA) in DMEM supplemented with 1% FBS and 1% P/S was added to the cells. After the agarose overlay solidified, the plates were returned to 37 °C and incubated for 5 days. Cells were fixed in 4% (vol/vol) formaldehyde in PBS for 1 h and stained with crystal violet (0.5% wt/vol in 25% methanol). Plaques were counted and analyzed using Quantity One software (Bio-Rad, Hercules, CA).

RNA purification and quantitative real-time PCR (qRT-PCR)

Total RNA was extracted from supernatant and cell pellet from DENV infected cultures using TRIzol reagent (Invitrogen, Carlsbad, CA) following the manufacturer's protocol. The One Step SYBR Ex Taq RT-PCR Kit (Takara, Clontech Laboratories, Inc., Mountain View, CA), designed for single step real-time RT-PCR using SYBR Green I detection, was utilized following the manufacturer's protocol. In brief, the 25 μl PCR mixture included 12.5 μl 2 × buffer (including dNTP mixture, Mg^{2+} and SYBR green I), 0.5 μl (2.5 unit) Ex Taq, 0.5 μl RTase mix, 0.5 μl 10 μM (final concentration 0.2 μM) forward primer (CTTAGGGTGGCAGGCTGTT), 0.5 μl 10 μM (final concentration 0.2 μM) reverse primer (CAGGGGAAGCTGGGTTGAC), 0.5 μl ROX reference dye II, 2.5 μl RNA sample, and 7.5 μl H_2O (Takara Bio Inc). The ten-fold serial dilutions of DENV-2 total RNA (10^3–10^7 copies/ml), prepared from DENV-2 stocks with known viral titer, were used as a reference for standard curve calculation. The mixtures were incubated in a 96-well optical plate (Applied BioSystems,), and qRT-PCR was carried out using StepOne Plus Real-Time PCR system (Applied Biosystems, Foster City, CA), following manufacturer's protocol. RT-PCR reaction performed as followings: reverse transcription was carried out by incubating mixture at 42 °C for 30 min and 95 °C for 5 min, followed by 40 PCR cycles: 95 °C for 10 s, 60 °C for 30 s, and completed by incubation at 95 °C for 15 s. The reaction was then incubated at 60 °C for 1 min and 95 °C for 15 s for melt curve. After the reaction, amplification curve and melting curve were verified, the standard curve established. The Ct value for each sample was determined by default threshold settings of the software.

Cell viability assay

Cell viability was determined using CellTiter-Glo (CTG) Luminescent cell viability assay (Promega, Madison, WI) as described previously (Che et al., 2009). Briefly, cells were seeded at 5000 cells/well in 96-well black plates with clear bottom using DMEM supplemented with 1% FBS, 1% P/S. After incubated overnight, cells were inoculated with DENV at designated MOI as noted in the text. The plates were then incubated at 37 °C with 5% CO_2 for 120 h to allow the development of CPE. Cell viability was measured at 120 h.p.i. using CTG reagent (Promega, Madison, WI) by adding equal volume (100 μl/well) of CTG reagent into each well. After 5 min incubation, relative luminescent signals were measured using Synergy 2 plate reader (BioTek Instruments Inc., Winooski, VT). Luminescent signal was normalized to that of control cells, and the percentages of cell viability were determined accordingly.

Protein sample preparation

Cell monolayers, with or without DENV infection, were washed twice with PBS and lysed on ice using lysis buffer (50 mM Tris, pH 7.4, 250 mM NaCl, 5 mM EDTA, 50 mM NaF, 1 mM Na_3VO_4, 1% Nonidet P40 (NP40), 0.02% NaN_3, 1% Triton X-100) (Invitrogen, Carlsbad, CA) supplemented with 1 mM PMSF and 1 × protease inhibitor mixture (Sigma-Aldrich, St. Louis, MO). The cell lysate was further incubated for 30 min on ice and vortex at 10 min interval. After centrifugation at 14,000*g* for 20 min at 4 °C, cell debris was discarded and supernatant was collected, aliquoted and stored in −80 °C. Protein concentration was determined using Bradford assay (Sigma-Aldrich, St. Louis, MO) prior to sodium dodecyl sulfate-polyacrylamide gel electrophoresis (SDS-PAGE).

Western blot analysis

Protein samples were boiled in 1 × loading buffer for 5 min prior to load into the SDS-PAGE gel. Proteins were separated in 10% SDS-PAGE at 150 V for 40 min. After transferred onto a PVDF membrane using Mini Trans-Blot cell (Bio-Rad, Hercules, CA), the membranes were blocked using 5% non-fat milk for 1 h at room temperature. Immunoblot analysis was performed using primary antibodies specific against each protein. Mouse monoclonal antibodies (mAbs) specifically against claudin-1 (D-4) was purchased from Santa Cruz biotechnology (Santa Cruz, CA). GAPDH, GST tag and HIS tag mAbs were purchased from GenScript (Piscataway, NJ). Goat anti-mouse IgG-HRP and rabbit anti-goat IgG-HRP were purchased from KPL Inc. (Gaithersburg, Maryland) and Southern Biotechnology Associates (Birmingham, AL), respectively. The ECL reagent (Millipore, Billerica, MA) was used for luminescence detection.

DNA transfection and rescue assay

Plasmids DNA were purified using PureLink quick plasmid midi-prep kit (Invitrogen, Carlsbad, CA), and concentration was quantified using Synergy 2 plate reader (BioTek Instruments Inc., Winooski, VT). For transfection, cells were seeded in 24-well plates at 80% confluence and transfected with 2 μg DNA/well using lipofectamine 2000 (Invitrogen, Carlsbad, CA), as described in manufacture's manual. After incubation at 37 °C for 6 h, transfecting medium was replaced with DMEM supplemented with 5% FBS. After incubated at 37 °C for another 48 h, cells were inoculated with DENV-2 at MOI of 1, or treated with compound 6 at concentration of 1 μM prior to inoculation. Cells were harvested and total RNA was extracted using TRIzol reagent at time points noted in the text, followed by qRT-PCR analysis for viral genomic RNA level as described above.

Indirect immunofluorescent assay (IFA)

Huh 7.5 cells with or without shRNA knockdown were seeded on chamber slides (Millipore, Billerica, MA). At desired time, cells were washed in PBS twice and fixed in 3.7% formaldehyde (Sigma-Aldrich, St. Louis, MO) at room temperature for 20 min. After being washed three times, cells were permeabilized in 0.2% Triton X-100 in PBS for 20 min. After blocking in 1% BSA in PBS for 1 h, cells were incubated with 200 μl anti-claudin-1 mAb (1:100) for 3 h. After three brief washes in 0.2% BSA in PBS, cells were incubated in goat anti-mouse IgG conjugated polyclonal antibody (1:500) for 1 h. Cells were then washed 5 times and mounted with cover slip using mounting medium (Vector Laboratories, Burlingame, CA), and examined using a Nikon fluorescence inverted microscope (Nikon, Tokyo, Japan).

Expression and purification of GST- and HIS-tagged recombinant proteins

The *E. coli* strain Rosetta (DE3) LysS (Novagen, Madison, WI) was transformed with pTriEx-4 or pGEX-3T4 expression plasmids by heat-shock method. Cells were cultured at 37 °C in LB medium supplemented with 100 μg/ml AMP until OD_{600} reached 0.6. To induce protein expression, 1 mM isopropylβ-D-thiogalactopyranoside (IPTG) was added into culture medium, followed by 4 h of culture at 30 °C. Cells were harvested by centrifuge at 6000*g* for 30 min at 4 °C, washed in PBS once and stored in −80 °C until purification. To purify HIS-tagged proteins, cells were re-suspended in ice-cold HIS-lysis buffer for HIS-tagged proteins (20 mM phosphate buffer pH 7.4, 10 mM imidazole, 0.5% Triton x-100, 250 mM NaCl). Cells were disrupted on ice using a sonic dismembrator (Fisher Scientific Company, Pittsburgh, PA). Cell debris was removed by spin at 1000*g* for 20 min at 4 °C. The inclusion bodies were collected by centrifugation at 8000*g* for 40 min at 4 °C and resuspended in 8 M urea buffer (8 M urea, 40 mM phosphate buffer, 10 mM imidazole, pH 7.4) with gentle rocking at 4 °C for 2 h. Suspension was centrifuged again at 8000*g* for 1 h at 4 °C, and supernatant with resolubilized proteins was collected and incubated with pre-equilibrated nickel chelate beads (GE Healthcare, Piscataway, NJ) for 2–3 h at 4 °C.

To purify GST-tagged proteins, supernatant was collected using GST-lysis buffer for GST-tagged proteins (1% Sarkosyl, 4.3 mM Na_2HPO_4, 1.47 mM KH_2PO_4, 0.137 M NaCl, 2.7 mM KCl, pH 7.3). After removal of the cell debris, supernatants were diluted 100 × using GST-wash buffer for GST-tagged proteins (4.3 mM Na_2HPO_4, 1.47 mM KH_2PO_4, 0.137 M NaCl, 2.7 mM KCl, 0.5% Triton x-100, pH 7.3), followed by incubation with pre-equilibrated Glutathione Sepharose 4B beads (GE Healthcare, Piscataway, NJ) for 4 h at 4 °C.

To further purify the HIS- and GST-tagged proteins, HIS and GST affinity beads were used (Bio-Rad, Hercules, CA). After incubate the affinity beads with the respective protein samples, the beads were loaded onto an empty column and proteins were purified following the manufacture's instruction. Briefly, beads were washed 5–10 times with 2 column volume (CV) of HIS-wash buffer for HIS-tagged proteins (20mM phosphate buffer pH 7.4, 250 mM NaCl, 50 mM imidazole), or GST-wash buffer for GST-tagged protein as described previously. Semi-purified proteins were eluted and collected in fifteen 1 ml fractions, using HIS elution buffer (20 mM phosphate buffer, 350 mM imidazole pH 7.4) for HIS-tagged proteins or GST elution buffer (10 mM reduced glutathione in 50 mM Tris–HCl, pH 8.0) for GST-tagged proteins. Fractions containing target proteins were analyzed using SDS-PAGE. Target proteins were then pooled from identified fractions and dialyzed against 20 mM phosphate buffer, 300 mM NaCl, 20% glycerol, at 4 °C overnight, using dialysis tubing with cut-off value

of 10 kDa. Dialysis product was then aliquoted and stored at −80 °C.

Pull-down assay

Total protein concentration of each purified recombinant protein was determined by Bradford assay (Sigma-Aldrich, St. Louis, MO). For in vitro pull-down assays, 12 μg of purified GST-prM was incubated with 1 mg purified HIS-tagged claudin-1 or its deletion mutations or point mutations in GST binding buffer (4.3 mM Na_2HPO_4, 1.47 mM KH_2PO_4, 0.137 M NaCl, 2.7 mM KCl, pH 7.3) at 4 °C with gentle rocking for overnight. A 50 μl pre-equilibrated Glutathione Sepharose 4B beads was added to the mixture and incubated for 4 h at 4 °C with gentle rocking. Subsequently, the binding mixture was loaded into micro-spin columns (Thermo-Pierce, Rockford, USA). Unbound proteins were removed by 6 washes of 500 μl GST binding buffer. The protein–protein complexes bound to Glutathione Sepharose 4B beads were eluted in 50 μl 1× GST elution buffer (10 mM reduced glutathione in 50 mM Tris–HCl, pH 8.0) by spin at 14,000*g* for 2 min. To analyze the pull-down result, 30 μl of each elution was subjected to SDS-PAGE analysis followed by immunoblotting with anti-claudin-1 monoclonal antibody (Santa Cruz, CA).

Statistical analysis

All data were analyzed using the GraphPad Prism program (GraphPad Software, San Diego, CA) and Microsoft Excel. Two-tailed Student's *t* tests were used to calculate *p* values.

Acknowledgment

This project was supported by the IMPACT funds from Department of Medicine at University of Alabama at Birmingham to Q. Li. We also thank the technical assistances from Dr. Linlin Gu and Mr. Zhijun Bai during the course of the work.

References

Andras, I.E., Toborek, M., 2011. HIV-1-induced alterations of claudin-5 expression at the blood-brain barrier level. Methods Mol. Biol. 762, 355–370.
Armstrong, S.M., Wang, C., Tigdi, J., Si, X., Dumpit, C., Charles, S., Gamage, A., Moraes, T.J., Lee, W.L., 2012. Influenza infects lung microvascular endothelium leading to microvascular leak: role of apoptosis and claudin-5. PLoS ONE 7, e47323.
Bartosch, B., Vitelli, A., Granier, C., Goujon, C., Dubuisson, J., Pascale, S., Scarselli, E., Cortese, R., Nicosia, A., Cosset, F.L., 2003. Cell entry of hepatitis C virus requires a set of co-receptors that include the CD81 tetraspanin and the SR-B1 scavenger receptor. J. Biol. Chem. 278, 41624–41630.
Benedicto, I., Molina-Jimenez, F., Bartosch, B., Cosset, F.L., Lavillette, D., Prieto, J., Moreno-Otero, R., Valenzuela-Fernandez, A., Aldabe, R., Lopez-Cabrera, M., Majano, P.L., 2009. The tight junction-associated protein occludin is required for a postbinding step in hepatitis C virus entry and infection. J. Virol. 83, 8012–8020.
Bielefeldt-Ohmann, H., Meyer, M., Fitzpatrick, D.R., Mackenzie, J.S., 2001. Dengue virus binding to human leukocyte cell lines: receptor usage differs between cell types and virus strains. Virus Res. 73, 81–89.
Che, P., Wang, L., Li, Q., 2009. The development, optimization and validation of an assay for high throughput antiviral drug screening against Dengue virus. Int. J. Clin. Exp. Med. 2, 363–373.
Cukierman, L., Meertens, L., Bertaux, C., Kajumo, F., Dragic, T., 2009. Residues in a highly conserved claudin-1 motif are required for hepatitis C virus entry and mediate the formation of cell–cell contacts. J. Virol. 83, 5477–5484.
da Silva Voorham, J.M., Rodenhuis-Zybert, I.A., Ayala Nunez, N.V., Colpitts, T.M., van der Ende-Metselaar, H., Fikrig, E., Diamond, M.S., Wilschut, J., Smit, J.M., 2012. Antibodies against the envelope glycoprotein promote infectivity of immature dengue virus serotype 2. PloS ONE 7, e29957.
Diamond, M.S., Edgil, D., Roberts, T.G., Lu, B., Harris, E., 2000. Infection of human cells by dengue virus is modulated by different cell types and viral strains. J. Virol. 74, 7814–7823.
Dickman, K.G., Hempson, S.J., Anderson, J., Lippe, S., Zhao, L., Burakoff, R., Shaw, R.D., 2000. Rotavirus alters paracellular permeability and energy metabolism in Caco-2 cells. Am. J. Physiol.—Gastrointest. Liver Physiol.279, G757–766.
Doig, A.J., Williams, D.H., 1991. Is the hydrophobic effect stabilizing or destabilizing in proteins? The contribution of disulphide bonds to protein stability. J. Mol. Biol.217, 389–398.
Evans, M.J., von Hahn, T., Tscherne, D.M., Syder, A.J., Panis, M., Wolk, B., Hatziioannou, T., McKeating, J.A., Bieniasz, P.D., Rice, C.M., 2007. Claudin-1 is a hepatitis C virus co-receptor required for a late step in entry. Nature 446, 801–805.
Fedwick, J.P., Lapointe, T.K., Meddings, J.B., Sherman, P.M., Buret, A.G., 2005. Helicobacter pylori activates myosin light-chain kinase to disrupt claudin-4 and claudin-5 and increase epithelial permeability. Infect. Immun. 73, 7844–7852.
Fujita, K., Katahira, J., Horiguchi, Y., Sonoda, N., Furuse, M., Tsukita, S., 2000. *Clostridium perfringens* enterotoxin binds to the second extracellular loop of claudin-3, a tight junction integral membrane protein. FEBS lett.476, 258–261.
Gao, F., Duan, X., Lu, X., Liu, Y., Zheng, L., Ding, Z., Li, J., 2010. Novel binding between pre-membrane protein and claudin-1 is required for efficient dengue virus entry. Biochem. Biophys. Res. Commun. 391, 952–957.
Gonzalez-Mariscal, L., Quiros, M., Diaz-Coranguez, M., Bautista P., 2012. Tight Junctions, Current Frontiers and Perspectives in Cell Biology, Prof. Stevo Najman (Ed.), ISBN: 978-953-51-0544-2, InTech.
Guevara Jr., J., Prashad, N., Ermolinsky, B., Gaubatz, J.W., Kang, D., Schwarzbach, A.E., Loose, D.S., Guevara, N.V., 2010. Apo B100 similarities to viral proteins suggest basis for LDL-DNA binding and transfection capacity. J. Lipid Res. 51, 1704–1718.
Guttman, J.A., Samji, F.N., Li, Y., Vogl, A.W., Finlay, B.B., 2006. Evidence that tight junctions are disrupted due to intimate bacterial contact and not inflammation during attaching and effacing pathogen infection in vivo. Infect. Immun. 74, 6075–6084.
Guzman, M.G., Halstead, S.B., Artsob, H., Buchy, P., Farrar, J., Gubler, D.J., Hunsperger, E., Kroeger, A., Margolis, H.S., Martinez, E., Nathan, M.B., Pelegrino, J.L., Simmons, C., Yoksan, S., Peeling, R.W., 2010. Dengue: a continuing global threat. Nat. Rev. Microbiol. 8, S7–16.
Halstead, S.B., Deen, J., 2002. The future of dengue vaccines. Lancet 360, 1243–1245.
Harris, H.J., Davis, C., Mullins, J.G., Hu, K., Goodall, M., Farquhar, M.J., Mee, C.J., McCaffrey, K., Young, S., Drummer, H., Balfe, P., McKeating, J.A., 2010. Claudin association with CD81 defines hepatitis C virus entry. J. Biol. Chem. 285, 21092–21102.
Heckman, K.L., Pease, L.R., 2007. Gene splicing and mutagenesis by PCR-driven overlap extension. Nat. Protocols2, 924–932.
Heinz, F.X., Allison, S.L., 2003. Flavivirus structure and membrane fusion. Adv. Virus Res. 59, 63–97.
Ip, P.P., Liao, F., 2010. Resistance to dengue virus infection in mice is potentiated by CXCL10 and is independent of CXCL10-mediated leukocyte recruitment. J. Immunol. 184, 5705–5714.
Jindadamrongwech, S., Smith, D.R., 2004. Virus overlay protein binding assay (VOPBA) reveals serotype specific heterogeneity of dengue virus binding proteins on HepG2 human liver cells. Intervirology 47, 370–373.
Kinney, R.M., Butrapet, S., Chang, G.J., Tsuchiya, K.R., Roehrig, J.T., Bhamarapravati, N., Gubler, D.J., 1997. Construction of infectious cDNA clones for dengue 2 virus: strain 16681 and its attenuated vaccine derivative, strain PDK-53. Virology 230, 300–308.
Krause, G., Winkler, L., Mueller, S.L., Haseloff, R.F., Piontek, J., Blasig, I.E., 2008. Structure and function of claudins. Biochim. et Biophys. Acta1778, 631–645.
Kuadkitkan, A., Wikan, N., Fongsaran, C., Smith, D.R., 2010. Identification and characterization of prohibitin as a receptor protein mediating DENV-2 entry into insect cells. Virology 406, 149–161.
Kuhn, R.J., Zhang, W., Rossmann, M.G., Pletnev, S.V., Corver, J., Lenches, E., Jones, C.T., Mukhopadhyay, S., Chipman, P.R., Strauss, E.G., Baker, T.S., Strauss, J.H., 2002. Structure of dengue virus: implications for flavivirus organization, maturation, and fusion. Cell 108, 717–725.
Li, J., Angelow, S., Linge, A., Zhuo, M., Yu, A.S., 2013. Claudin-2 pore function requires an intramolecular disulfide bond between two conserved extracellular cysteines. Am. J. Physiol.—Cell Physiol..
Lindenbach, B.D., Rice, C.M., 2003. Molecular biology of flaviviruses. Adv. Virus Res. 59, 23–61.
Liu, S., Kuo, W., Yang, W., Liu, W., Gibson, G.A., Dorko, K., Watkins, S.C., Strom, S.C., Wang, T., 2010. The second extracellular loop dictates Occludin-mediated HCV entry. Virology 407, 160–170.
Liu, S., Yang, W., Shen, L., Turner, J.R., Coyne, C.B., Wang, T., 2009. Tight junction proteins claudin-1 and occludin control hepatitis C virus entry and are down-regulated during infection to prevent superinfection. J. Virol. 83, 2011–2014.
Lorenza González-Mariscal, M.Q., Bautista, P., M.D.-C., Tight Junctions.
Lozach, P.Y., Burleigh, L., Staropoli, I., Navarro-Sanchez, E., Harriague, J., Virelizier, J.L., Rey, F.A., Despres, P., Arenzana-Seisdedos, F., Amara, A., 2005. Dendritic cell-specific intercellular adhesion molecule 3-grabbing non-integrin (DC-SIGN)-mediated enhancement of dengue virus infection is independent of DC-SIGN internalization signals. J. Biol. Chem. 280, 23698–23708.
Mackenzie, J.M., Westaway, E.G., 2001. Assembly and maturation of the flavivirus Kunjin virus appear to occur in the rough endoplasmic reticulum and along the secretory pathway, respectively. J. Virol. 75, 10787–10799.
McKeating, J.A., Zhang, L.Q., Logvinoff, C., Flint, M., Zhang, J., Yu, J., Butera, D., Ho, D.D., Dustin, L.B., Rice, C.M., Balfe, P., 2004. Diverse hepatitis C virus glycoproteins mediate viral infection in a CD81-dependent manner. J. Virol. 78, 8496–8505.

Meertens, L., Bertaux, C., Cukierman, L., Cormier, E., Lavillette, D., Cosset, F.L., Dragic, T., 2008. The tight junction proteins claudin-1, -6, and -9 are entry cofactors for hepatitis C virus. J. Virol. 82, 3555–3560.
Mercado-Curiel, R.F., Black, W.C.T., Munoz Mde, L., 2008. A dengue receptor as possible genetic marker of vector competence in Aedes aegypti. BMC Microbiol. 8, 118.
Miller, J.L., de Wet, B.J., Martinez-Pomares, L., Radcliffe, C.M., Dwek, R.A., Rudd, P.M., Gordon, S, 2008. The mannose receptor mediates dengue virus infection of macrophages. PLoS Pathog. 4, e17.
Mrsny, R.J., Brown, G.T., Gerner-Smidt, K., Buret, A.G., Meddings, J.B., Quan, C., Koval, M., Nusrat, A., 2008. A key claudin extracellular loop domain is critical for epithelial barrier integrity. Am. J. Pathol. 172, 905–915.
Murray, J.M., Aaskov, J.G., Wright, P.J., 1993. Processing of the dengue virus type 2 proteins prM and C-prM. J. Gen. Virol. 74 (Pt 2), 175–182.
Nava, P., Lopez, S., Arias, C.F., Islas, S., Gonzalez-Mariscal, L., 2004. The rotavirus surface protein VP8 modulates the gate and fence function of tight junctions in epithelial cells. J. Cell Sci. 117, 5509–5519.
Navarro-Sanchez, E., Altmeyer, R., Amara, A., Schwartz, O., Fieschi, F., Virelizier, J.L., Arenzana-Seisdedos, F., Despres, P., 2003. Dendritic-cell-specific ICAM3-grabbing non-integrin is essential for the productive infection of human dendritic cells by mosquito-cell-derived dengue viruses. EMBO Rep. 4, 723–728.
Obert, G., Peiffer, I., Servin, A.L., 2000. Rotavirus-induced structural and functional alterations in tight junctions of polarized intestinal Caco-2 cell monolayers. J. Virol. 74, 4645–4651.
Perera, R., Kuhn, R.J., 2008. Structural proteomics of dengue virus. Curr. Opin. Microbiol. 11, 369–377.
Pileri, P., Uematsu, Y., Campagnoli, S., Galli, G., Falugi, F., Petracca, R., Weiner, A.J., Houghton, M., Rosa, D., Grandi, G., Abrignani, S., 1998. Binding of hepatitis C virus to CD81. Science 282, 938–941.
Ploss, A., Evans, M.J., Gaysinskaya, V.A., Panis, M., You, H., de Jong, Y.P., Rice, C.M., 2009. Human occludin is a hepatitis C virus entry factor required for infection of mouse cells. Nature 457, 882–886.
Reyes-Del Valle, J., Chavez-Salinas, S., Medina, F., Del Angel, R.M., 2005. Heat shock protein 90 and heat shock protein 70 are components of dengue virus receptor complex in human cells. J. Virol. 79, 4557–4567.
Reyes-del Valle, J., Del Angel, R.M., 2004. Isolation of putative dengue virus receptor molecules by affinity chromatography using a recombinant E protein ligand. J. Virol. Methods 116, 95–102.
Rodenhuis-Zybert, I.A., Moesker, B., da Silva Voorham, J.M., van der Ende-Metselaar, H., Diamond, M.S., Wilschut, J., Smit, J.M., 2011. A fusion-loop antibody enhances the infectious properties of immature flavivirus particles. J. Virol. 85, 11800–11808.
Rodenhuis-Zybert, I.A., van der Schaar, H.M., da Silva Voorham, J.M., van der Ende-Metselaar, H., Lei, H.Y., Wilschut, J., Smit, J.M., 2010. Immature dengue virus: a veiled pathogen? PLoS Pathog. 6, e1000718.
Sakaguchi, T., Kohler, H., Gu, X., McCormick, B.A., Reinecker, H.C., 2002. Shigella flexneri regulates tight junction-associated proteins in human intestinal epithelial cells. Cell. Microbiol.4, 367–381.
Salas-Benito, J., Reyes-Del Valle, J., Salas-Benito, M., Ceballos-Olvera, I., Mosso, C., Del Angel, R.M., 2007. Evidence that the 45-kD glycoprotein, part of a putative dengue virus receptor complex in the mosquito cell line C6/36, is a heat-shock related protein. Am. J. Trop. Med. Hyg. 77, 283–290.
Scarselli, E., Ansuini, H., Cerino, R., Roccasecca, R.M., Acali, S., Filocamo, G., Traboni, C., Nicosia, A., Cortese, R., Vitelli, A., 2002. The human scavenger receptor class B type I is a novel candidate receptor for the hepatitis C virus. EMBO J. 21, 5017–5025.
Sonoda, N., Furuse, M., Sasaki, H., Yonemura, S., Katahira, J., Horiguchi, Y., Tsukita, S., 1999. Clostridium perfringens enterotoxin fragment removes specific claudins from tight junction strands: evidence for direct involvement of claudins in tight junction barrier. J. Cell Biol.147, 195–204.
Stiasny, K., Fritz, R., Pangerl, K., Heinz, F.X., 2009. Molecular mechanisms of flavivirus membrane fusion. Amino Acids.
Takahashi, A., Kondoh, M., Masuyama, A., Fujii, M., Mizuguchi, H., Horiguchi, Y., Watanabe, Y., 2005. Role of C-terminal regions of the C-terminal fragment of Clostridium perfringens enterotoxin in its interaction with claudin-4. J. Controlled Release: Off. J. Controlled Release Soc. 108, 56–62.
Taniyama, Y., Kuroki, R., Omura, F., Seko, C., Kikuchi, M., 1991. Evidence for intramolecular disulfide bond shuffling in the folding of mutant human lysozyme. J. Biol. Chem. 266, 6456–6461.
Tassaneetrithep, B., Burgess, T.H., Granelli-Piperno, A., Trumpfheller, C., Finke, J., Sun, W., Eller, M.A., Pattanapanyasat, K., Sarasombath, S., Birx, D.L., Steinman, R.M., Schlesinger, S., Marovich, M.A., 2003. DC-SIGN (CD209) mediates dengue virus infection of human dendritic cells. J. Exp. Med. 197, 823–829.
van der Schaar, H.M., Rust, M.J., Chen, C., van der Ende-Metselaar, H., Wilschut, J., Zhuang, X., Smit, J.M., 2008. Dissecting the cell entry pathway of dengue virus by single-particle tracking in living cells. PLoS Pathog. 4, e1000244.
Van Itallie, C.M., Anderson, J.M., 2006. Claudins and epithelial paracellular transport. Annu. Rev. Physiol. 68, 403–429.
Van Itallie, C.M., Betts, L., Smedley 3rd, J.G., McClane, B.A., Anderson, J.M., 2008. Structure of the claudin-binding domain of *Clostridium perfringens* enterotoxin. J. Biol. Chem. 283, 268–274.
Wang, Q.Y., Patel, S.J., Vangrevelinghe, E., Xu, H.Y., Rao, R., Jaber, D., Schul, W., Gu, F., Heudi, O., Ma, N.L., Poh, M.K., Phong, W.Y., Keller, T.H., Jacoby, E., Vasudevan, S.G., 2009. A small-molecule dengue virus entry inhibitor. Antimicrob. Agents Chemother. 53, 1823–1831.
Wang, S., He, R., Anderson, R., 1999. PrM- and cell-binding domains of the dengue virus E protein. J. Virol. 73, 2547–2551.
Waninger, S., Kuhen, K., Hu, X., Chatterton, J.E., Wong-Staal, F., Tang, H., 2004. Identification of cellular cofactors for human immunodeficiency virus replication via a ribozyme-based genomics approach. J. Virol. 78, 12829–12837.
Wen, H., Watry, D.D., Marcondes, M.C., Fox, H.S., 2004. Selective decrease in paracellular conductance of tight junctions: role of the first extracellular domain of claudin-5. Mol. Cell. Biol.24, 8408–8417.
WHO, 2012. Dengue and severe dengue fact sheet ⟨http://www.who.int/mediacentre/factsheets/fs117/en/⟩. The Journal of General Virology 87, pp. 1075–1084.
Yu, I.M., Holdaway, H.A., Chipman, P.R., Kuhn, R.J., Rossmann, M.G., Chen, J., 2009. Association of the pr peptides with dengue virus at acidic pH blocks membrane fusion. J. Virol. 83, 12101–12107.
Yu, I.M., Zhang, W., Holdaway, H.A., Li, L., Kostyuchenko, V.A., Chipman, P.R., Kuhn, R.J., Rossmann, M.G., Chen, J., 2008. Structure of the immature dengue virus at low pH primes proteolytic maturation. Science 319, 1834–1837.
Yuhan, R., Koutsouris, A., Savkovic, S.D., Hecht, G., 1997. Enteropathogenic *Escherichia coli*-induced myosin light chain phosphorylation alters intestinal epithelial permeability. Gastroenterology 113, 1873–1882.
Zhang, Y., Corver, J., Chipman, P.R., Zhang, W., Pletnev, S.V., Sedlak, D., Baker, T.S., Strauss, J.H., Kuhn, R.J., Rossmann, M.G., 2003. Structures of immature flavivirus particles. EMBO J. 22, 2604–2613.
Zhang, Y., Zhang, W., Ogata, S., Clements, D., Strauss, J.H., Baker, T.S., Kuhn, R.J., Rossmann, M.G., 2004. Conformational changes of the flavivirus E glycoprotein. Structure 12, 1607–1618.
Zheng, A., Yuan, F., Li, Y., Zhu, F., Hou, P., Li, J., Song, X., Ding, M., Deng, H., 2007. Claudin-6 and claudin-9 function as additional coreceptors for hepatitis C virus. J. Virol. 81, 12465–12471.
Zybert, I.A., van der Ende-Metselaar, H., Wilschut, J., Smit, J.M., 2008. Functional importance of dengue virus maturation: infectious properties of immature virions. J. Gen. Virol. 89, 3047–3051.